https://doi.org/10.20965/ijat.2023.p0032

Research Paper:

Effects of Bit Shape of Electroplated Diamond Tool Used for Drilling Small Diameter Holes in Glass Plate on Machining Fluid Flow and Chip Discharge

Tappei Oyamada, Akira Mizobuchi[†], and Tohru Ishida

Tokushima University

2-1 Minamijosanjima-cho, Tokushima-city, Tokushima 770-8506, Japan

[†]Corresponding author, E-mail: a-mizobuchi@tokushima-u.ac.jp

[Received June 30, 2022; accepted September 22, 2022]

Our laboratory has been exploring the development of tools for drilling holes in glass plates, and the drilling techniques to be adopted for it. A devised tool shape that could prevent the occurrence of cracks at the exit holes achieved high quality through hole drilling of 100 holes or more using only the drilling cycle. However, crack-free drilling beyond this number of holes cannot be performed. This is due to the adhesion of the residual chip on the tool surface when the number of holes increases. Therefore, further improvement of chip discharge is needed to achieve crack-free drilling. In this report, we consider that chip discharge results from the flow of the machining fluid. To investigate the cause of chip discharge, we analyzed the flow of the machining fluid in the hole using computational fluid dynamics and the supposed chip discharge conditions. The results obtained in this study are summarized as follows. (1) In the case of a cylindrical tool, the Z-axis directional flow of the machining fluid did not occur in the hole. This is because the tool does not have bumps to agitate the fluid on the side, and the gap between the tool and the inner surface of the hole is narrow. (2) The plate side widened the gap between the tool and inner surface of the hole. Therefore, the fluid was likely to flow in the Z-axis direction in the hole. (3) For the tool with the plane side bit, the flow entered the hole from one plane side and exited the hole from the other plane side. (4) When the tool end is spherical, the Z-axis directional flow of the fluid occurs at the tool end. (5) The fluid flow of the devised tool weakened as the drilling depth increased. To improve the chip discharge performance of the designed tool, the Z-axis directional flow of the machining fluid must occur in an area deeper than 2 mm.

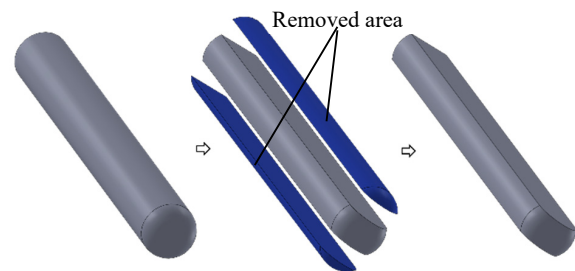**Keywords:** tool bit shape, machining fluid, chip, drilling, glass plate

Fig. 1. Schematic diagram of the designed tool bit.

1. Introduction

When a cylindrical grinding wheel mounted on a shaft is used for drilling holes in a glass plate, the pores between the grains act as chip pockets, but the pocket volume is small. In addition, the gap between the grinding wheel and the inside surface of the hole is narrow, and there is almost no escape for the chip. Therefore, it is difficult for the chip to discharge out of the hole and it tends to adhere to the tool as the machining progresses. Drilling by the tool of chip adhesion causes deterioration of the machining quality and tool breakage. Therefore, the chip discharge method is crucial. In general, the chip discharge method is a step-machining method and an ultrasonic vibration method [1–12]. However, these methods have disadvantages, such as lower machining efficiency and capital investment costs.

In our laboratory, we have been exploring the development of tools for drilling holes in glass plates to achieve high machining quality, high machining efficiency, and low machining cost, as well as the drilling techniques to be adopted for it [13–16]. **Fig. 1** shows the shape of the designed tool. The tool end of the cylindrical shaft, made of cemented carbide, is hemispherical. The thrust force when the tool penetrates the glass plate decreases slowly, thereby preventing cracking. In addition, two plane surfaces are placed opposite to each other on the cylindrical surface of the shaft, creating a large chip storage space between the plane surface and the inside surface of the hole. The unique feature of the tool is the spontaneous
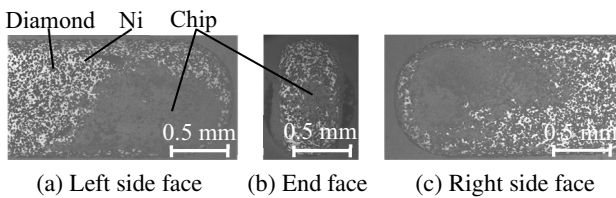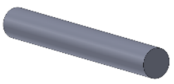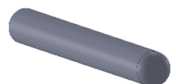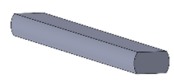
Effects of Bit Shape of Electroplated Diamond Tool
Used for Drilling Small Diameter Holes in Glass Plate on
Machining Fluid Flow and Chip Discharge

(a) Left side face   (b) End face   (c) Right side face
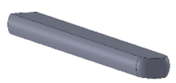
Fig. 2. Chip adhesion condition on the designed tool after drilling.

Table 1. Model of tool bit shape.

(a) Vertical section

(b) Horizontal section   (c) Horizontal section mesh

Fig. 3. Analytical model.

discharge of the chip from the chip storage space, and chip discharge is performed without the general measures mentioned above. However, the chip adhered to the tool as the number of holes increased, as shown in **Fig. 2**. One of the causes of chip adhesion is the material properties of the machining fluid [17–19]. We considered other factors also.

In this study, we consider that chip discharge results from the flow of the machining fluid. To investigate the cause of the chip not being discharged, we analyzed the flow of the machining fluid in the hole using computational fluid dynamics (CFD) and the supposed chip discharge conditions.

2. Analysis Conditions

An analysis was performed on the commercial tool shape and the invented tool shape. **Table 1** lists shapes of tool model. Two cylindrical tool models with different end-face shapes were used in the analysis, as commercial tools. For the invented tool, two tool models with different end-face shapes with a straight face on the tool side were used in the analysis. Based on this, the tool was named a circle flat end (CF), circle ball end (CB), rectangle flat end (RF), and rectangle ball end (RB). The first letter represents the first letter of the radial cross-sectional shape of the tool. C indicates a circle and R indicates a rectangle. The short sides of the RF and RB have curves but are considered straight lines. The second letter is the first letter of the tool bit shape. F indicates a flat end and B indicates a ball end. The machining fluid flow occurring by the four
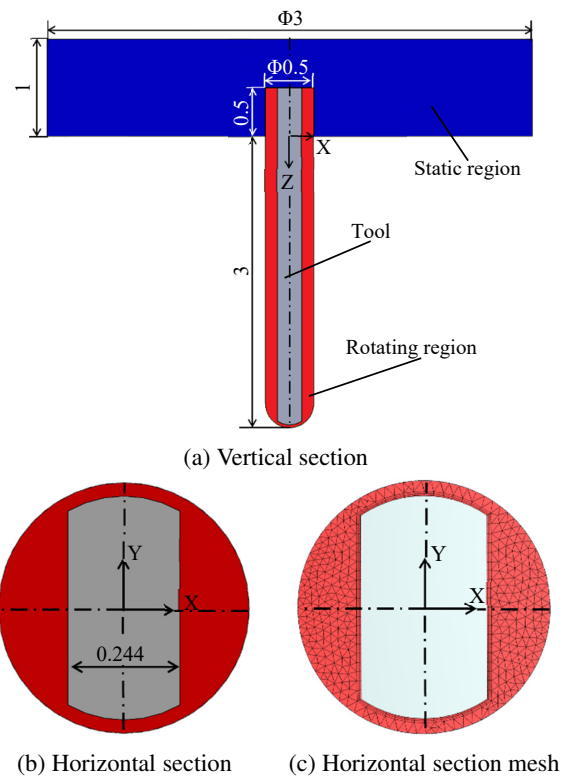
types of tools in the holes was analyzed.

In this study, fluid flow was analyzed using computational fluid dynamics software (Autodesk CFD 2021, Autodesk). **Fig. 3** shows the analytical model. The tool end on the entrance hole side was fixed to the static region. A rotating region that imitates the machining fluid is positioned to cover the tool. The static region was treated as an incompressible fluid and had a water physical property value at the water temperature of 293 K. The analytical conditions were set to provide an incompressible fluid and k–ε turbulence model. The fluid flow when the tool rotates at 30000 rpm was analyzed. The origin was located at the center of the hole entrance. The analysis interval was 1×10^{-4} s.

3. Tool Bit Shape and Machining Fluid Flow

3.1. Machining Fluid Flow by Tool Without Plane Side Bit

Figures 4 and **5** show the distribution of flow velocity and the Z-axis direction flow velocity in the radial cross section for CF and CB respectively. The fluid in both holes rotated in the same direction as that of the tool. The farther away from the center of the hole, the faster is the flow in the rotation direction. The numbers of revolutions per minute of the fluid and tool were identical. The relative position of the fluid with respect to the tool does not vary in the XY plane. In other words, the tool and the fluid rotate together. By contrast, in the distribution
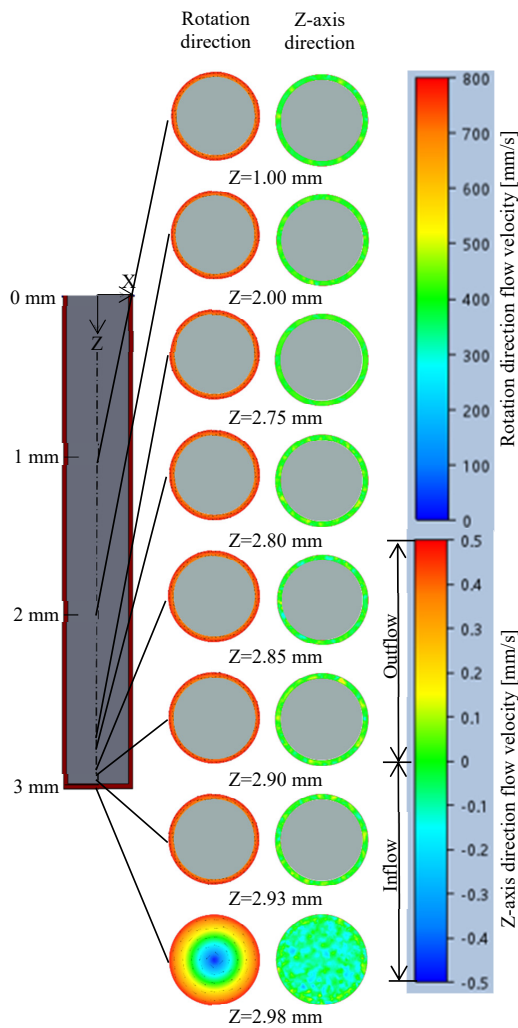
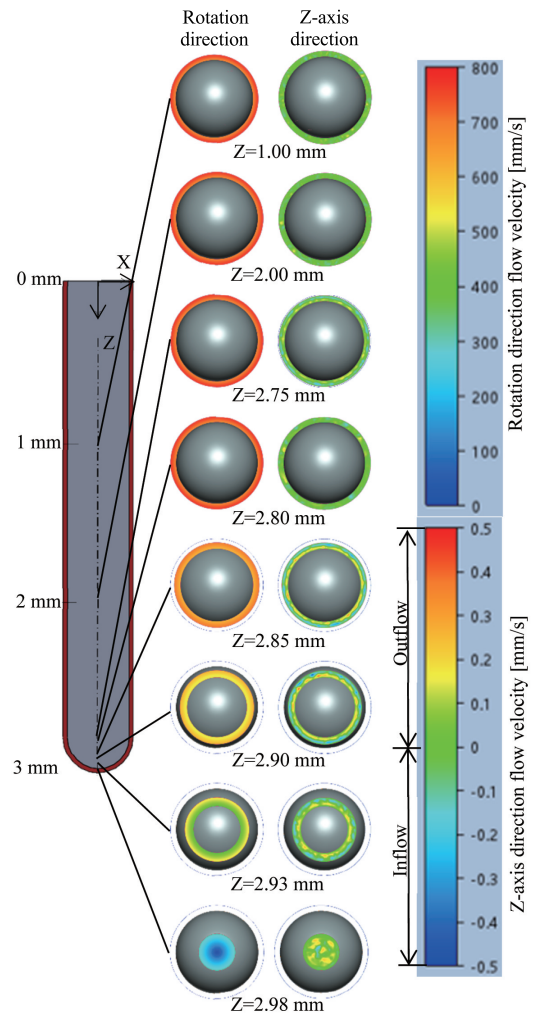**Fig. 4.** Distribution of flow velocity of CF.

Fig. 5. Distribution of flow velocity of CB.

of the Z-axis direction flow velocity, the Z-axis direction flow did not occur in the entire hole. In CF and CB, the fluid rotates with the tool but does not flow in the Z-axis direction; thus, it stagnates at a certain hole depth. The fluid did not circulate through the holes. This is because CF and CB do not have bumps on their sides to agitate the fluid. Furthermore, fluid flow in the direction of the Z-axis does not easily occur in the hole because the gap between the tool and the inside surface of the hole is narrow as the tool occupies most of the volume of the hole. Therefore, for the CF and CB, it is difficult for the chip to discharge out of the hole because the machining fluid does not circulate in and out of the hole.

3.2. Machining Fluid Flow by Tool with Plane Side Bit

Figures 6 and **7** show the analysis results for RF and RB, respectively. The fluid rotated in the same direction as the tool in CF and CB, and its velocity increased as it moved away from the center of rotation. The number of rotations of the fluid and tool matched. The relative position of the fluid with respect to the tool does not vary

in the XY plane for the CF and CB. In other words, the tool and the fluid rotate together. The Z-axis direction flow occurred at a depth of 0–1.00 mm in the distribution of the Z-axis direction flow for the RF. This flow entered the hole from one straight side and exited from the other straight side. The plate side widened the gap between the tool and inner surface of the hole. For this reason, the fluid is likely to flow in the direction of the Z-axis in the hole. The fluid circulates at a depth of 0–1.00 mm due to the Z-axis direction flow. Therefore, the machining fluid circulated from a drilling depth of 0–1 mm. Furthermore, this flow carried the chip out of the hole. On the other hand, after the drilling depth of 1 mm, the Z-axis flow of machining fluid occurred there is no flow in the Z-axis direction, and the machining fluid does not circulate. The deeper the drilling depth, the lower the circulation of the machining fluid. It is likely that the machining fluid could not discharge the chip outside the hole.

In the distribution of the Z-axis velocity for the RB, the Z-axis direction flow occurred at a drilling depth of 0–2.00 mm. The Z-axis direction flow of the machining fluid for RB was more active than that for RF, and the flow area was wider. In addition, flow in the Z-axis direction
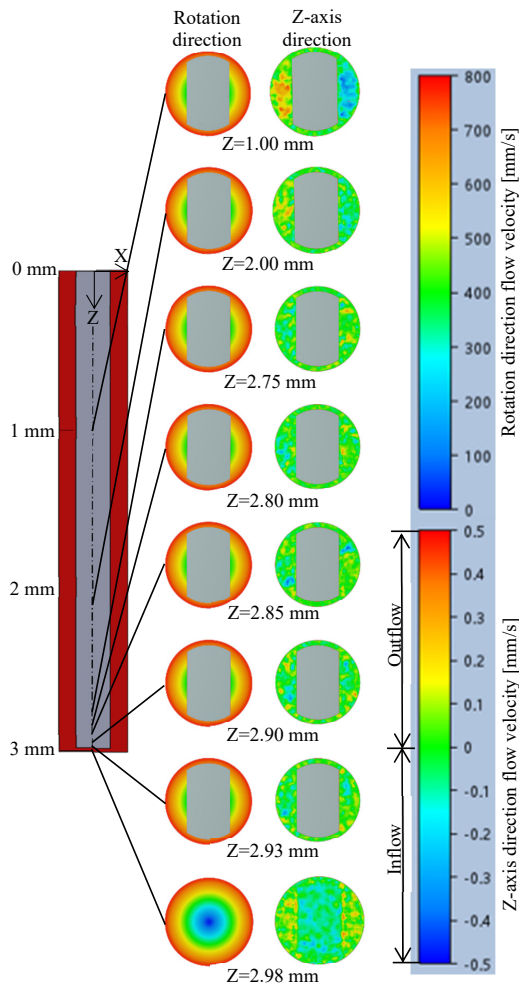
Effects of Bit Shape of Electroplated Diamond Tool
Used for Drilling Small Diameter Holes in Glass Plate on
Machining Fluid Flow and Chip Discharge

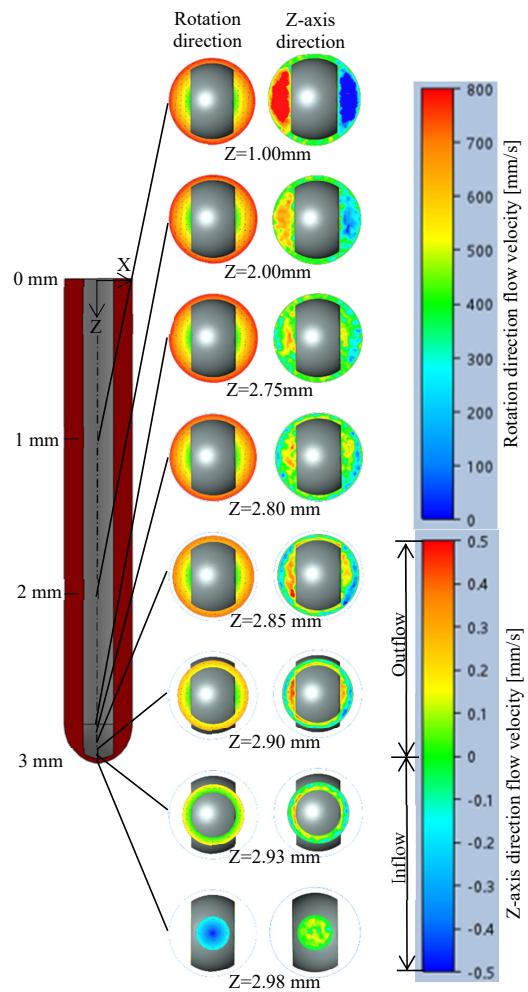**Fig. 6.** Distribution of flow velocity of RF.

Fig. 7. Distribution of flow velocity of RB.

also occurred at drilling depths of 2.75–2.90 mm. At this depth, the outflow direction flow occurred near the plane sides, and the inflow direction flow occurred near the inside surface of the hole. The Z-axis flow was conducive to chip discharge. In the case of drilling with the RB, the Z-axis machining fluid flow occurring at the tool end circulated from the hole entrance to near the bottom of the hole and discharged the chip. The tool shape designed in our laboratory is advantageous for the chip discharge.

3.3. Consideration of the Cause of Machining Fluid Flow in the Z-axis Direction

Based on the analysis results in the previous sections, no Z-axis flow occurred in the machining fluid in the CF and CB of the cylindrical tools. In contrast, RF and RB, which have straight planes on the tool sides, produced flow in the Z-axis direction. The following is a discussion of the causes. The Taylor vortex is considered the cause of the Z-axis directional flow in the processing fluid. A Taylor vortex is generated in a double cylinder with a rotating inner cylinder [20]. The fluid near the inner cylinder flows toward the outer cylinder owing to the centrifugal force, thereby generating a vortex. The Z-axis flow of the machining fluid did not occur in the CF and CB. The gap

between the tool and hole is too small, which prevents the Taylor vortex from being generated and the circulation of the machining fluid from occurring. The Z-axis flow of the machining fluid occurred in the RF and RB. The straight plane of the tool side widened the gap between the tool and hole wall, and the machining fluid circulated. Only for RB, where the tool end is curved, flow in the Z-axis direction occurred near the tool end. Different tool end shapes have different hole bottom shapes. The RF forms a cylindrical hole, and the bottom and sides of the hole are perpendicular. The RB formed a hole with a curve, at the bottom and surface. Because the shape of the hole-side surface differs between RF and RB, the fluid flowing to the hole-side surface owing to the rotation of the tool shows different flows. In RF, the hole sides are perpendicular to the flow; therefore, the flow that reaches the sides of the hole is considered to be less likely to move in the vertical direction of the hole. However, in RB, the flow reaching the hole side is more likely to move toward the vertical direction of the hole because the side of the hole is curved, and vortexes are more likely to be generated. Therefore, in the RB, a Z-axis flow was generated near the tool end.
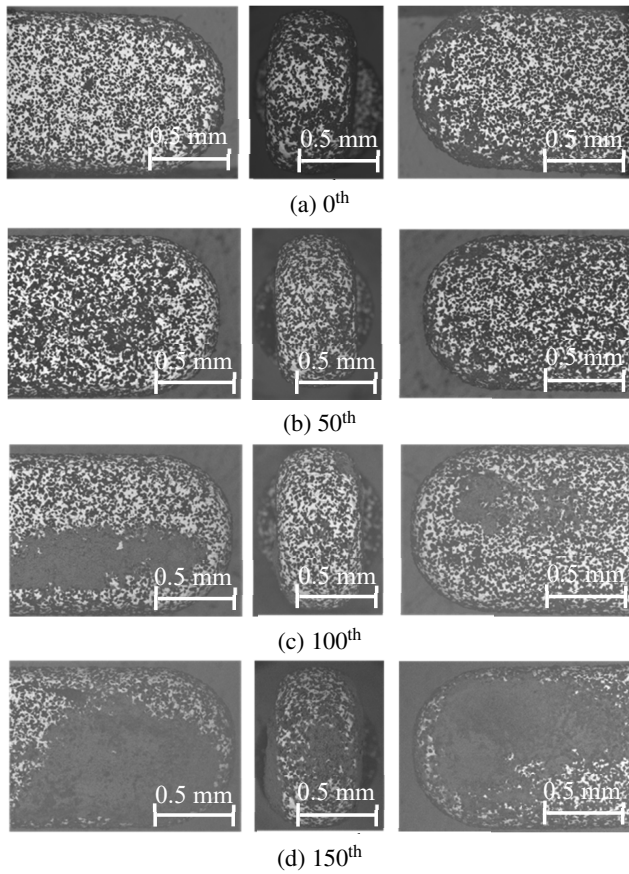
(a) 0th

(b) 50th

(c) 100th

(d) 150th

Fig. 8. Progress of chip adhesion of RB.

(a) A-A   (b) B-B

Fig. 9. Distribution of flow velocity at the Z-axis direction.

4. Chip Adhesion to Tool and Machining Fluid Flow

The four tools were used to machine soda-lime glass with a diameter of 1.0 mm and a depth of 3 mm. CF, CB, and RF break during machining. **Fig. 8** shows the chip adhesion progress of RB as the number of drilled holes increased. The drilling conditions were set to a cutting speed of 47 m/min (spindle speed of 15000 rpm) and feed rate of 1 mm/min. The analysis results in the previous section showed that the RB tool had a shape that facilitated the chip discharge. However, the residual chip in the hole adhered to the straight side of the tool along with an increase in the number of holes. When the number of drilled holes reached 100, chip adhesion occurred on the tool-plane sides. More chips adhered to one side and fewer chips adhered to the other. When the number of drilling holes reached 150, chip adhesion occurred on the tool-edge surface and plane sides.

Figure 9 shows the distribution of the Z-axis direction flow velocity in the cross section parallel to the plane side for the RB. The fluid flowed into the hole from one plane and out of the hole from the other plane. If the flow of the machining fluid governs the chip discharge, the chip is more likely to be discharged from the plane side where outflow occurs. We consider this to be the cause of the differen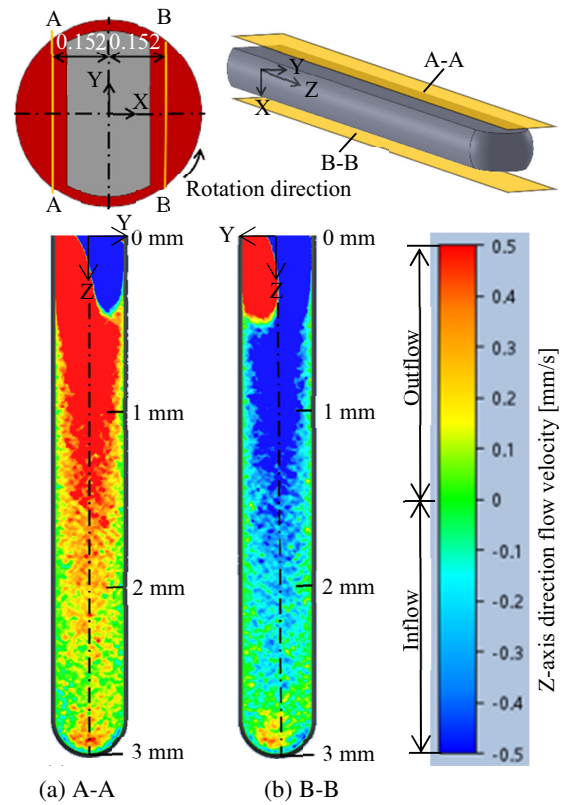ce in the amount of chip adhesion on the two sides of the plane, as shown in **Fig. 8**. Then, as the number of machined holes increased, the chip adhered to the plane side where fluid outflow occurred, and the chip blocked the discharge destination. Consequently, the gap between the tool and the inner surface of the hole became narrower, as in the CB, making it difficult for the machining fluid to flow, and the flow of the machining fluid inside the hole became stagnant. The chip began to adhere to the plane side, where the amount of chip adhesion was small. The Z-axis directional flow of the machining fluid up to a drilling depth of 2 mm was actively present in both the inflow and outflow. However, after a depth of 2 mm, the Z-axis direction flow of the machining fluid did not occur, except at the end. The Z-axis direction flow at the tool end was active at the tool end but became negative as it approached the other end. The greater the drilling depth, the poorer the chip discharge performance of the RB tool. Next, deep-hole drilling is performed using the RB tool to investigate the chip discharge conditions.

5. Chip Discharge Condition of RB During Deep Hole Drilling

The RB tool was used machine soda-lime glass with a diameter of 0.5 mm and a depth of 5 mm. The drilling conditions were set to a cutting speed of 47 m/min (spindle speed of 30000 rpm) and a feed rate of 1 mm/min. The tool broke when the second hole was processed. The
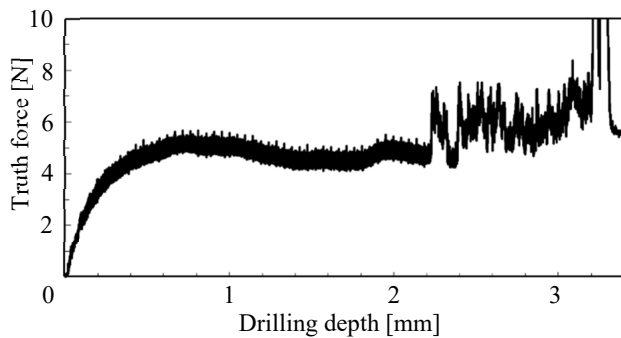
Effects of Bit Shape of Electroplated Diamond Tool
Used for Drilling Small Diameter Holes in Glass Plate on
Machining Fluid Flow and Chip Discharge

Fig. 10. Relationship between drilling depth and thrust force.

following is a discussion of the state of the chip discharge based on the behavior of the thrust force, referring to the results of previous thrust force research [14]. **Fig. 10** shows the relationship between the drilling depth and thrust force. The thrust force increased gradually from the start of machining to a drilling depth of 0.8 mm and remained constant from 0.8 mm to 2.2 mm. This force increased and decreased intensely from 2.2 to 3.2 mm depth. When the depth reached approximately 3.2 mm, this force increased and decreased rapidly, and then no longer fluctuated. The tool broke, and the glass shattered. The results obtained from our previous research [14] show an intense increase and decrease in the thrust force owing to residual chips in the hole. The chips were discharged from the start of the processing to a depth of 2.2 mm. Beyond this depth, the chip was not discharged and adhered to the tool, thereby inhibiting machining. In **Fig. 9**, this depth is almost the same as the depth at which the flow is stagnant in the Z-axis direction. The deeper the drilling depth, the more difficult it is for the machining fluid to flow, and the poorer is the chip discharge condition.

6. Improved Chip Discharge of the Devised Tool

In the analysis in this study, the protrusion and distribution of abrasive grains in the tool were not considered. Therefore, the same flow as the analysis results did not occur during machining. However, we infer that the flow of the machining fluid is similar to that of the analytical results for two reasons. (1) In **Fig. 9**, the fluid flows into the hole from one straight face and out of the hole from the other straight face. It is considered that chips tend to be discharged from the straight face where flow in the outflow direction occurs. **Fig. 8** shows that the number of chips that adhered to the tool differed between the two straight surfaces. (2) In **Figs. 9** and **10**, the hole depth where the Z-axis directional flow of the machining fluid was less likely to occur matched the hole depth where the thrust force began to shift intensely up and down. Therefore, the analysis results were close to the actual flow of the machining fluid without considering the protrusion and distribution of the abrasive grains.

The analysis results show that the RB tool produced circulation of the machining fluid in the region of 0–2 mm hole depth and in the region of 2.75–2.90 mm hole depth, which is the tool end. The chips are discharged from the tool drilling area by circulation at the end of the tool. They were then discharged from the machined hole by circulation at hole depths of 0–2 mm. However, as shown in **Fig. 9**, when the tool end reaches a hole depth of 2 mm or greater, an area with no circulation occurs between the two circulation flows, making chip discharge difficult. To prevent chip adhesion to the tool and achieve higher machining efficiency, it is necessary to circulate the machining fluid even after a hole depth of 2 mm.

7. Conclusions

In this study, we considered that chip discharge results from the flow of the machining fluid. To investigate whether the chip was not discharged, we analyzed the flow of the machining fluid in the hole using computational fluid dynamics and the supposed chip discharge conditions. The results obtained in this study are summarized as follows.

(1) In the case of the cylindrical tool, the Z-axis directional flow of the machining fluid did not occur in the hole. This was because the tool did not have bumps to agitate the fluid on the side, and the gap between the tool and the inside surface of the hole was narrow.

(2) The plate side widened the gap between the tool and inner surface of the hole. Therefore, the fluid was likely to flow in the Z-axis direction in the hole.

(3) For the tool with a plane side bit, the flow entered the hole from one plane side and exited the hole from the other plane side.

(4) In the case of the ball end, the Z-axis directional flow of the fluid occurred at the tool bit.

(5) The fluid flow of the devised tool weakened as the drilling depth increased. To improve the chip discharge performance of the designed tool, it is necessary for the Z-axis direction flow of the machining fluid to occur in areas deeper than 2 mm.

References:
[1] C. Nash and M. Rahman, "Effect of machining parameters in ultrasonic vibration cutting," Int. J. of Machine Tools & Manufacture, Vol.48, No.9, pp. 965-974, 2018.
[2] D. Sindhu, L. Thakur, and P. Chandna, "Parameter optimization of rotary ultrasonic machining on quartz glass using response surface methodology (RSM)," Silicon, Vol.12, No.3, pp. 629-643, 2020.
[3] J. Wang, J. Zhang, P. Feng, and P. Guo, "Damage formation and suppression in rotary ultrasonic machining of hard and brittle materials: A critical review," Ceramics Int., Vol.44, No.2, pp. 1227-1239, 2018.
[4] K. Egashira, R. Kumagai, R. Okina, K. Yamaguchi, and M. Ota, "Drilling of microholes down to 10 μm in diameter using ultrasonic grinding," Precision Engineering, Vol.38, No.3, pp. 605-610, 2014.

[5] K. Egashira and T. Masuzawa, "Microultrasonic machining by the application of workpiece vibration," CIRP Annals, Vol.48, No.1, pp. 131-134, 1999.

[6] K. Noma, Y. Kakinuma, T. Aoyama, and S. Hamada, "Ultrasonic vibration-assisted machining of chemically strengthened glass with workpiece bending," J. of Advanced Mechanical Design, Systems, and Manufacturing, Vol.9, No.2, JAMDSM0016, 2015.

[7] K. Noma, Y. Takeda, T. Aoyama, Y. Kakinuma, and S. Hamada, "High-precision and high-efficiency micromachining of chemically strengthened glass using ultrasonic vibration," Procedia CIRP, Vol.14, pp. 389-394, 2014.

[8] P. Fernando, M. Zhang, Z. Pei, and W. Cong, "Intermittent and continuous rotary ultrasonic machining of K9 glass: an experimental investigation," J. of Manufacturering and Materials Processing, Vol.20, No.1, pp. 605-610, 2017.

[9] R. Tsuboi, Y. Kakinuma, T. Aoyama, H. Ogawa, and S. Hamada, "Ultrasonic vibration and cavitation-aided micromachining of hard and brittle materials," Procedia CIRP, Vol.1, pp. 342-346, 2012.

[10] T. Kuriyagawa, T. Shirosawa, O. Saitoh, and K. Syoji, "Development of micro ultrasonic abrasive machining system (1st report, studies in micro ultrasonic abrasive machining)," Int. J. Series C: Mechanical Systems, Machine Elements and Manufacturing, Vol.45, No.2, pp. 593-600, 2002.

[11] Y. Nambu, K. Ochiai, K. Horio, J. Kaneko, T. Watanabe, and S. Matsuda, "Attempt to increase step feed by adding ultrasonic vibration in micro deep drilling," J. of Advanced Mechanical Design, Systems, and Manufacturing, Vol.5, No.2, pp. 129-138, 2011.

[12] Y. Chen, X. Feng, and G. Xin, "Experimental study on ultrasonic vibration-assisted WECDM of glass microstructures with a high aspect ratio," Micromachines, Vol.12, No.2, 125, 2021.

[13] A. Mizobuchi, H. Ogawa, and M. Masuda, "Drilling conditions and crack restaint of step drilling method in through-hole drilling of glass plate," J. of the Japan Society for Precision Engineering, Vol.77, No.3, pp. 296-300, 2011 (in Japanese).

[14] A. Mizobuchi, I. Tada, and T. Ishida, "Development of electroplated diamond tool for fracture size minimization in miniature drilling of glass plate," J. of the Japan Society for Abrasive Technology, Vol.58, No.5, pp. 321-327, 2014 (in Japanese).

[15] A. Mizobuchi, Y. Kagawa, and T. Ishida, "Miniature drilling of chemically stengthened glass plate using electroplated diamond tool," Int. J. Automation Technol., Vol.10, No.5, pp. 780-785, 2016.

[16] A. Mizobuchi, M. S. A. Aziz, R. Izamshah, and T. Ishida, "Chip discharge performance of micro-hole drilling through a glass plate using an electroplated diamond tool with different drill bits," Int. J. of Precision Engineerring and Manufacturing, Vol.19, No.9, pp. 1273-1280, 2018.

[17] A. Mizobuchi, K. Honda, and T. Ishida, "Improved chip discharge in drilling of glass plate using back tapered electroplated diamond tool," Int. J. of Precision Engineerring and Manufacturing, Vol.18, No.9, pp. 1197-1204, 2017.

[18] K. Honda, A. Mizobuchi, and T. Ishida, "Investigation of grinding fluid for prevention of chip adhesion in miniature drilling of glass plate using electroplated diamond tool," Key Engineering Materials, Vol.749, pp. 52-57, 2017.

[19] K. Honda, A. Mizobuchi, and T. Ishida, "Prevention of chip adhesion by acting non-ionic surfactant physical properties," J. of the Japan Socirty for Abrasive Technology, Vol.62, No.6, pp. 324-329, 2018 (in Japanese).

[20] P. R. Fenstermacher, H. L. Swinner, and J. P. Gollub, "Dynamical instabilities and the transition to chaotic Taylor vortex flow," J. of Fluid Mechanics, Vol.94, No.1, pp. 103-128, 1979.

Name:
Tappei Oyamada

Affiliation:
Graduate School of Science and Technology, Tokushima University

Address:
2-1 Minamijosanjima-cho, Tokushima-city, Tokushima 770-8506, Japan
Brief Biographical History:
2021 Received Bachelor of Science and Technology from Tokushima University
Membership in Academic Societies:
● Japan Society for Abrasive Technology (JSAT)

Name:
Akira Mizobuchi

ORCID:
0000-0003-4937-089X

Affiliation:
Associate Professor, Graduate School of Technology, Industrial and Social Sciences, Tokushima University

Address:
2-1 Minamijosanjima-cho, Tokushima-city, Tokushima 770-8506, Japan
Brief Biographical History:
1999- Research Associate, Tokushima University
2007- Assistant Professor, Tokushima University
2013- Associate Professor, Tokushima University
Main Works:
● "Improved Chip Discharge in Drilling of Glass Plate Using Back Tapered Electroplated Diamond Tool," Int. J. of Precision Engineering and Manufacturing, Vol.18, No.9, pp. 1197-1204, 2017.
● "Prevention of chip adhesion by acting non-ionic surfactant physical properties," J. of the Japan Society for Abrasive Technology, Vol.62, No.6, pp. 324-329, 2018 (in Japanese).
● "Mechanics of Slag Control in Gas Cutting of Steel Plate by Slag Pasting," J. of Japan Society for Design Engineering, Vol.55, No.1, pp. 33-42, 2020.
● "Slag Sticking Suppression in Gas Cutting of Steel Plate by Carbon-added Paste," J. of Japan Society for Design Engineering, Vol.55, No.11, pp. 673-680, 2020 (in Japanese).
● "Optimization of Wet Grinding Conditions of Sheets Made of Stainless Steel," J. of Manufacturing and Materials Processing, Vol.4, No.4, 114, 2020.
● "Polishing Performance of a Recycled Grinding Wheel Using Grinding Wheel Scraps for the Wet Polishing of Stainless-Steel Sheets," Int. J. Automation Technol., Vol.16, No.1, pp. 60-70, 2022.
Membership in Academic Societies:
● Japan Society of Mechanical Engineers (JSME)
● Japan Society for Precision Engineering (JSPE)
● Japan Society for Abrasive Technology (JSAT)
● Japan Society of Electro-Machining Engineers (JSEME)
● Japan Society for Design Engineering (JSDE)

Effects of Bit Shape of Electroplated Diamond Tool
Used for Drilling Small Diameter Holes in Glass Plate on
Machining Fluid Flow and Chip Discharge

Name:
Tohru Ishida

Affiliation:
Professor, Department of Mechanical Science,
Graduate School of Technology, Industrial and
Social Sciences, Tokushima University

Address:
2-1 Minamijosanjima-cho, Tokushima-city, Tokushima 770-8506, Japan
Brief Biographical History:
1999- Research Associate, The University of Electro-Communications
2003- Assistant Professor, Osaka University
2008- Associate Professor, Osaka University
2011- Professor, Tokushima University
Main Works:
● "Development of CAD/CAM System for Cross Section's Changing Hole
Electrical Discharge Machining —Formulation of Post Processor—," J. of
Advanced Mechanical Design, Systems, and Manufacturing (JAMDSM),
Vol.4, No.5, pp. 1054-1065, 2010.
● "Design and Implementation of Automatic Discharge Gap Controller for
a Curved Hole Creating Microrobot with an Electrical Discharge
Machining Function," Int. J. Automation Technol., Vol.4, No.6,
pp. 542-551, 2010.
● "Fundamental Study on Hole Fabrication inside a Hole by Means of
Electrical Discharge Machining," Int. J. Automation Technol., Vol.8, No.5,
pp. 773-782, 2014.
Membership in Academic Societies:
● Japan Society of Mechanical Engineers (JSME)
● Japan Society for Precision Engineering (JSPE)